

SANDIA REPORT

SAND2007-2791

Unlimited Release

Printed August 2007

Mobility Analysis Tool Based on the Fundamental Principle of Conservation of Energy

Calvin (HyukChul) Nho, Jon R. Salton, Barry Spletzer

Prepared by
Sandia National Laboratories
Albuquerque, New Mexico 87185 and Livermore, California 94550

Sandia is a multiprogram laboratory operated by Sandia Corporation,
a Lockheed Martin Company, for the United States Department of Energy's
National Nuclear Security Administration under Contract DE-AC04-94AL85000.

Approved for public release; further dissemination unlimited.

Issued by Sandia National Laboratories, operated for the United States Department of Energy by Sandia Corporation.

NOTICE: This report was prepared as an account of work sponsored by an agency of the United States Government. Neither the United States Government, nor any agency thereof, nor any of their employees, nor any of their contractors, subcontractors, or their employees, make any warranty, express or implied, or assume any legal liability or responsibility for the accuracy, completeness, or usefulness of any information, apparatus, product, or process disclosed, or represent that its use would not infringe privately owned rights. Reference herein to any specific commercial product, process, or service by trade name, trademark, manufacturer, or otherwise, does not necessarily constitute or imply its endorsement, recommendation, or favoring by the United States Government, any agency thereof, or any of their contractors or subcontractors. The views and opinions expressed herein do not necessarily state or reflect those of the United States Government, any agency thereof, or any of their contractors.

Printed in the United States of America. This report has been reproduced directly from the best available copy.

Available to DOE and DOE contractors from
U.S. Department of Energy
Office of Scientific and Technical Information
P.O. Box 62
Oak Ridge, TN 37831

Telephone: (865) 576-8401
Facsimile: (865) 576-5728
E-Mail: reports@adonis.osti.gov
Online ordering: <http://www.osti.gov/bridge>

Available to the public from
U.S. Department of Commerce
National Technical Information Service
5285 Port Royal Rd.
Springfield, VA 22161

Telephone: (800) 553-6847
Facsimile: (703) 605-6900
E-Mail: orders@ntis.fedworld.gov
Online order: <http://www.ntis.gov/help/ordermethods.asp?loc=7-4-0#online>



SAND2007-2791
Unlimited Release
Printed August 2007

Mobility Analysis Tool Bases on the Fundamental Principle of Conservation of Energy

Calvin (HyukChul) Nho, Jon R. Salton, Barry Spletzer
Intelligent Systems, Robotics, and Cybernetics Group
Intelligent Systems Controls Department
Sandia National Laboratories
P.O. Box 5800
Albuquerque, NM 87185

Abstract

In the past decade, a great deal of effort has been focused in research and development of versatile robotic ground vehicles without understanding their performance in a particular operating environment. As the usage of robotic ground vehicles for intelligence applications increases, understanding mobility of the vehicles becomes critical to increase the probability of their successful operations. This paper describes a framework based on conservation of energy to predict the maximum mobility of robotic ground vehicles over general terrain. The basis of the prediction is the difference between traction capability and energy loss at the vehicle-terrain interface.

The mission success of a robotic ground vehicle is primarily a function of mobility. Mobility of a vehicle is defined as the overall capability of a vehicle to move from place to place while retaining its ability to perform its primary mission. A mobility analysis tool based on the fundamental principle of conservation of energy is described in this document. The tool is a graphical user interface application.

The mobility analysis tool has been developed at Sandia National Laboratories, Albuquerque, NM. The tool is at an initial stage of development. In the future, the tool will be expanded to include all vehicles and terrain types.

Table of Contents

1	Nomenclature.....	6
2	Introduction.....	9
3	General Overview of the Theory	9
3.1	Energy Method to Mobility Analysis of Vehicles.....	10
3.2	Mobility Analysis of a Vehicle Over Deformable Soils.....	13
3.3	Pressure-Sinkage Relation of Homogenous and Deformable Terrain.....	13
3.4	Dissipation Energy Due to Deformation of Terrain	15
3.5	Shear Stress-Shear Deformation Relation of Homogenous and Deformable Terrain ..	16
3.6	Distribution of Stresses at the Contact Area.....	17
3.7	Distribution of the Stresses Under Wheels in the Tandem Configuration.....	19
3.8	Depth of the Track Mark.....	20
3.9	Traction Energy Capability from Terrain	20
3.10	Mobility Analysis Algorithms	21
4	Mobility Analysis Tool.....	21
4.1	Overall Picture	21
4.2	The Input Panel.....	24
4.2.1	Defining Terrain Characteristic Parameters.....	24
4.2.2	Defining Obstacle Characteristic Parameters	25
4.2.3	Defining Vehicle Characteristic Parameters.....	25
4.3	Menu items.....	25
5	Conclusion	26
6	References.....	27
7	Distribution.....	28

List of Figures

Figure 1:	Vehicle Traveling Over Terrain.....	10
Figure 2:	Soil Classification Defined by USDA Soil Textural Triangle.....	14
Figure 3:	Pressure-Sinkage Relation of Various Homogeneous and Deformable Soils with 1.6 inch Penetration Plates	15
Figure 4:	Mohr-Coulomb Soil Failure Criterion.....	16
Figure 5:	Description of Stresses Acting on Wheels	17
Figure 6:	Stresses Acting on the Wheels in a Tandem Configuration.....	20
Figure 7:	Mobility Analysis Tool at Startup.....	22
Figure 8:	Mobility Analysis Tool Showing Mobility Prediction Display	23
Figure 9:	Tabs in the Input Panel.....	24

1 Nomenclature

A_{plate}	Area of a pressure-sinkage plate
b	Smaller dimension of contact patch, width of rectangular contact area, radius of circular contact area, or width of a tire/track
C	Cohesion term in Mohr-Coulomb soil failure criterion
E_d	Dissipation energy, Extended Conservation of energy
$E_{d,terrain}$	Dissipation energy from the deformation of a terrain
$E_{d,tire}$	Dissipation energy from the deformation of tires
$E_{d,trak}$	Dissipation energy from the deformation of tracks
$E_{d,friction}$	Dissipation energy from the friction between a vehicle and a terrain
E_{gain}	Total inflow of energy into a vehicle, Extended Conservation of energy
E_{loss}	Total outflow of energy from a vehicle, Extended Conservation of energy
E_{tc}	Traction energy capability, Extended Conservation of energy
$E_{tc,terrain}$	Traction energy capability from the maximum shearing resistance of a terrain
$E_{tc,vehicle}$	Traction energy capability from the maximum shearing resistance of tires/tracks
$E_{tc,friction}$	Traction energy capability from the maximum friction between tires/tracks and a terrain
F_L	Load due to the weight of a vehicle
g	Acceleration due to gravity
h	Elevation change of the center of gravity of a vehicle
i	Index representing the i^{th} wheel from the front of a vehicle
i_s	Slip of a tire over a terrain
j_{sd}	Shear deformation of a terrain
K	Shear deformation coefficient in shear stress-shear deformation relation of terrain
k_c	Cohesive coefficient of the pressure-sinkage relation of terrain
k_s	Lumped coefficient of the pressure-sinkage relation of terrain
k_ϕ	Frictional coefficient of the pressure-sinkage relation of terrain
l	Length of track mark or length of the path a vehicle travels
m	Mass of a vehicle
n	Exponent of pressure-sinkage relation of terrain
p_h	Pressure on a pressure-sinkage plate
r	Radius of a tire
T	Torque available at the traction system in a vehicle

v_f	Final speed of a vehicle
v_i	Initial speed of a vehicle
<i>Work</i>	Work done by a plate to create an indentation in a terrain
x_0	Displacement along the longitudinal axes from the vertical axes at which a tire makes contact with a terrain
z	Vertical displacement
z_0	Depth of a track mark, sinkage depth of a plate
z_p	Compounded depth of a track mark caused by wheels in a tandem configuration from the leading wheel to the $(i - 1)^{th}$ wheel
ΔE	Change in energy within a vehicle, Conservation of energy
ΔKE	Change in kinetic energy within a vehicle
ΔPE	Change in potential energy within a vehicle
ϕ	Angle of internal shearing resistance of a terrain
ϑ	Slope of a terrain
θ	Angular displacement
θ_0	Angle from the vertical axes at which a tire makes contact with a terrain
θ_m	Angle from the vertical axes at which a tire creates the maximum radial stress on a terrain
θ_r	Angle from the vertical axes at which a tire breaks contact with a terrain
σ	Normal stress or radial stress
τ	Shear stress or tangential stress
τ_{max}	Maximum shear strength of a terrain

2 Introduction

In recent years it has become increasingly clear that small robots provide a needed capability to the warfighter. In Iraq soldiers are using and depending on small robots daily but only in situations that are controlled and pose a serious risk of injury or death [1]. As these robots become more autonomous and mobile, their role will be more significant. Furthermore, understanding their mobility is important for the proper selection of vehicle configuration and design parameters to meet specific operational requirements.

Predicting the mobility capability of ground robotic vehicles over general terrain is a largely unsolved problem. In contrast, many researchers and developers in military and civilian vehicles have studied the mobility of off-road vehicles since the mid 20th century. The most well-known mobility models are the NATO Reference Mobility Model (NRMM) [7] and the Bekker mobility model [7]. The NRMM is based on the empirical correlation between dimensionless performance parameters of tires or tracks and the cone index of terrain measured from a cone penetrometer. Because of its original intent to be used for specific large scale, manned vehicles (i.e. – specific tanks and trucks), it is not easily extended to smaller scale (i.e. – PACKBOT size) generic unmanned/robotic ground vehicles.

The Bekker mobility model is based on Bekker's widely cited three text books, which stimulated interest in the systematic development of the principle of land locomotion mechanics [2-4]. The model is based on estimations of normal and shear stresses exerted by an off-road vehicle using pressure-sinkage and shear stress-shear deformation relations of terrain developed from bevameter measurements. The method then applies a force balance method to predict the mobility. Many researchers like Janosi [3], Wong [5], Iagnemma and Dubowsky [6] follow this footprint with a modified and refined mobility model.

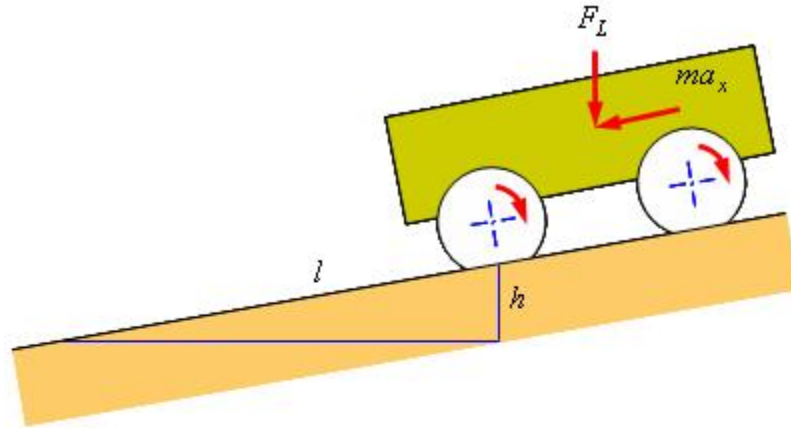
In this paper, a mobility analysis of robotic ground vehicles over general terrain is discussed. This analysis is based on the fundamental principle of conservation of energy and the Bekker terrain characteristic relations (the pressure-sinkage and shear stress-shear deformation relations). The development of a mobility tool based on these methods and its user interface is also discussed.

3 General Overview of the Theory

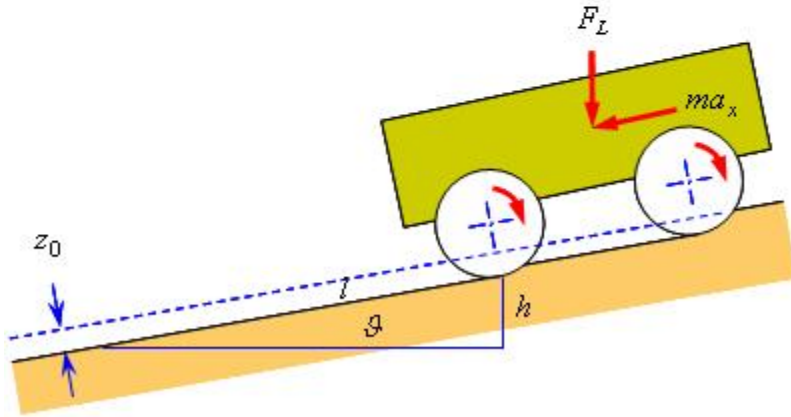
The mobility algorithms used in the mobility analysis tool are developed based on the fundamental principle of conservation of energy. According to Wikipedia (a free internet encyclopedia), the fundamental principle of conservation of energy states that "the total inflow of energy into a system must equal to the total outflow of energy from the system, plus the change in the energy contained within the system." The principle is a powerful tool for solving problems in mechanics. In this section, mobility algorithms based on the conservation of energy principle for describing mobility capabilities of vehicle over a generic terrain are discussed in detail.

3.1 Energy Method to Mobility Analysis of Vehicles

When a vehicle travels over terrain, according to the principle of conservation of energy, the total inflow of energy (E_{gain}) into the vehicle must equal the total outflow of energy



(a) Vehicle Traveling Over Concrete Road



(b) Vehicle Traveling Over Soft Deformable Terrain

Figure 1: Vehicle Traveling Over Terrain

(E_{loss}) from the vehicle, plus the change in the energy (ΔE) contained within the vehicle. Thus, the energy relation of the vehicle is given by

$$E_{gain} = E_{loss} + \Delta E \quad (1)$$

Figure 1 shows a vehicle traveling over a concrete road (a) and over a soft deformable terrain (b). For the vehicle, the change in the energy contained within the vehicle is comprised of change in kinetic energy (ΔKE) and change in potential energy (ΔPE). For vehicles that are assumed to have a constant weight, the change of the kinetic energy is caused by a change in velocity which is due to acceleration and deceleration of the vehicle. The change of the potential energy is caused by an elevation change of the center of gravity which is due to climbing/descending

sloped terrain or obstacles. Then, the change of the energy contained within the vehicle is given by

$$\begin{aligned}\Delta E &= \Delta KE + \Delta PE \\ &= \frac{1}{2} m(v_f^2 - v_i^2) + mg\Delta h\end{aligned}\quad (2)$$

where m denotes constant mass of the vehicle, v_f and v_i denote the final and initial velocity of the vehicle, g denotes gravity of earth, and Δh denotes an elevation change of the center of gravity, which is positive when the vehicle moves away from the center of earth.

The total outflow of energy (E_{loss}) from a vehicle is the amount of energy that is lost to the environment. This includes heat losses from the engine, inefficiencies in the drive train, and traction losses. The energy loss as part of an energy efficiency analysis of vehicles is not the focus of the mobility algorithms. The focus of the mobility algorithms is to predict the mobility capabilities of vehicles by applying the principle of conservation of energy at the traction system of a vehicle with an assumption that unlimited torque is available at the traction system. The unlimited torque can be positive (driven wheel), negative (braking wheel), and zero (free rolling). The traction system interacts with terrain in order to create traction energy, but also, loses energy due to the interaction. The term, dissipation energy (E_d), is used to differentiate the total outflow of energy from the traction system to the total outflow of energy from the vehicle. The following is a list of factors that can contribute to the dissipation energy:

- Soft and deformable terrain ($E_{d,terrain}$) – When a vehicle travels over soft and deformable terrain, the vehicle will leave a track mark on the terrain. An amount of energy is transferred from the vehicle to the terrain in order to create the track mark. A deeper track mark implies greater dissipation energy.
- Tire deformation ($E_{d,tire}$) – Energy loss caused by hysteresis in tire materials due to the deflection of the tire while rolling over terrain. A larger tire deformation implies greater dissipation energy.
- Track deformation ($E_{d,track}$) – Energy loss caused by hysteresis in track materials due to the deflection of the track rotating around a track traction system and interacting with the terrain. There are two distinctive deformations of a track. One is caused by the arrangement of drive wheels and idler wheels such that the track is required to maintain a certain shape while rotating around them. The other is caused by the interaction between the track and terrain. A larger track deformation implies greater dissipation energy.
- Friction ($E_{d,friction}$) – Energy loss caused by friction between the vehicle and terrain. There are several scenarios in which friction can occur. When wheels or tracks of a vehicle lock, this creates sliding friction between wheels/tracks and terrain. Whenever the body of a vehicle contacts terrain or obstacles, this creates a sliding friction.

Including these factors into the total outflow of energy at the traction system produces the following relation:

$$E_{loss} = E_d = E_{d,terrain} + E_{d,tire} + E_{d,track} + E_{d,friction} \quad (3)$$

The total inflow of energy (E_{gain}) into a vehicle is an amount of energy gain which will be used by the vehicle to do useful tasks, i.e. climb a sloped terrain, negotiate obstacles, etc. Like the energy loss described in the previous paragraph, the focus of the mobility algorithms is the energy gain at the contact area between wheels/tracks and terrain. The traction energy capability (E_{tc}) is used to describe the energy gain. When a driving torque is applied to drive wheels of the traction system in a vehicle, a shearing stress is developed at the contact area of the tires/tracks and terrain. The traction energy capability of the vehicle depends on the shear stress. There are three factors that limit the maximum traction energy capability. They are:

- Maximum shearing resistance of the terrain ($E_{tc,terrain}$) – The traction energy capability of the vehicle cannot be greater than the traction energy computed from the maximum shearing resistance of the terrain.
- Maximum shearing resistance of the tire/track ($E_{tc,vehicle}$) – The traction energy capability of the vehicle cannot be greater than the traction energy computed from the maximum shearing resistance of the tire/track.
- Maximum friction between the tire/track and terrain ($E_{tc,friction}$) – The traction energy capability of the vehicle cannot be greater than the traction energy computed from the maximum friction between the tire/track and terrain.

The traction energy capability of a vehicle is determined by the minimum of these three traction energy capabilities, and it is written as:

$$E_{tc} = \min(E_{tc,terrain}, E_{tc,vehicle}, E_{tc,friction}) \quad (4)$$

For example, the traction energy capability will be dictated by the terrain shearing resistance when a vehicle travels over a dry and deformable terrain because the terrain will fail before it reaches the maximum friction. As another example, the traction energy capability will be dictated by the maximum friction when a vehicle travels over a concrete road because it will reach the maximum friction before it will tear off the concrete road or the tires. In addition, the traction energy capability can be negative if braking torque is applied at the drive wheels of the traction systems instead of the driving torque.

Using these energies, the mobility capability of a vehicle over terrain can be analyzed. Combining previously defined energy terms, the energy relation given by equation (1) can be rewritten as:

$$E_{tc} = E_d + \frac{1}{2}m(v_f^2 - v_i^2) + mgh \quad (5)$$

Based on equation (5), one can predict whether a vehicle can travel over a terrain or not. If the traction energy capability of the vehicle is greater than the sum of the dissipation energy and change in potential energy, then the vehicle can travel over the terrain. Otherwise, the vehicle cannot travel over the terrain. More information can be extracted from the relationship, i.e.

minimum travel time from one place to another, maximum acceleration or deceleration, etc. Also, the equation can be used to estimate the maximum slope the vehicle can climb for a given terrain.

The most important factors for developing effective and accurate mobility algorithms based on the energy method are an identification of energies involved in the operation of a vehicle over terrain and the development of analytic expressions for the identified energies. A more detailed example of the mobility analysis of a wheeled vehicle over a soft and deformable terrain based on the energy method will be given in the following subsection. Some of the dissipation energies and the traction energy capability will be described in detail through an example.

3.2 *Mobility Analysis of a Vehicle Over Deformable Soils*

The dissipation energies and the traction energy capability highly depend on the characteristic behaviors of terrain, tires, tracks and the body of a vehicle at the contact area. The focus of this section is on developing expressions for the identified energies involved when a vehicle travels over a deformable terrain. A development of mobility algorithms based on the energy method is illustrated through a simple case study. A vehicle with two axles and the same tire on each end of the axles is chosen for the illustration, and a soft and deformable soil is chosen to see the mobility capabilities of the vehicle over the soil. For the purpose of the illustration, the deflection of the tires is ignored by assuming that the tires are highly pressurized. The vehicle travels over the soil as shown in Figure 1(b). According to conservation of energy, the energy relation during the operation of the vehicle is given by:

$$\begin{aligned} E_{tc,terrain} &= E_{d,terrain} + \frac{1}{2}m(v_f^2 - v_i^2) + mgh \\ &= E_{d,terrain} + \frac{F_L}{2g}(v_f^2 - v_i^2) + F_L l \sin(\vartheta) \end{aligned} \quad (6)$$

where F_L denotes the load due to the weight of the vehicle, l denotes the length of the path the vehicle travels, and ϑ denotes the slope of the soil. According to equation (6), mobility capabilities of the vehicle over the soil can be predicted, if the dissipation energy due to the deformation of terrain and the traction energy capability from terrain are known. In order to develop analytical expressions, the pressure-sinkage and shear stress-shear deformation relations of terrain developed by Bekker [1 and 2] are adopted to describe the terrain behaviors.

3.3 *Pressure-Sinkage Relation of Homogenous and Deformable Terrain*

The most well-known pressure-sinkage relation of a homogenous terrain is the one given by Bekker [1]. The relation describes the vertical strength of terrain for a given set of vertical stresses on the contact surface. Bekker described the relation by the following equation:

$$p_h(z) = k_s \cdot z^n \quad (7)$$

where $p_h(z)$ denotes pressure, z denotes sinkage, and k_s and n denote the coefficients of the relation obtained from experimental data. For a given plate, sinkage of the plate increases as

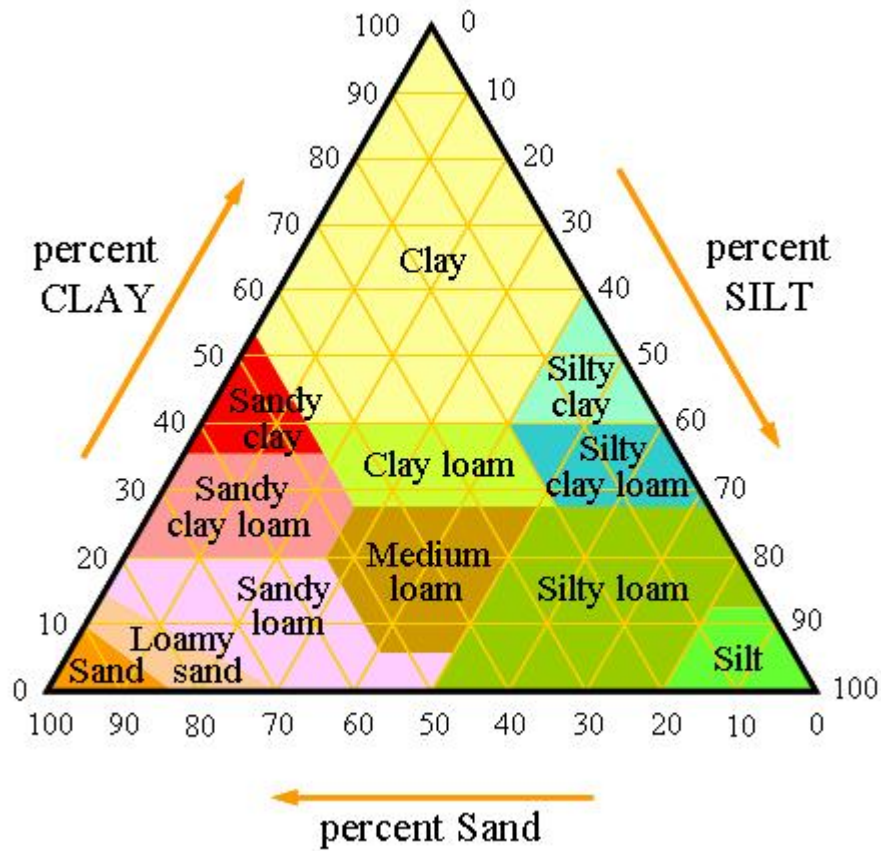


Figure 2: Soil Classification Defined by USDA Soil Textural Triangle

pressure increases, and the amount of sinkage depends on the two coefficients, k_s and n . The coefficient n has a range from 0.1 to 1.6 depending on the type of soils and their conditions. Typical values of n are 0.2 for clay, 1.1 for dry sand and 1.6 for snow. Bekker showed that the k_s depends on the smaller dimension of the plate, and it is given by:

$$k_s = \frac{k_c}{b} + k_\phi \quad (8)$$

where b denotes the smaller dimension of the contact patch, that is the width of a rectangular contact area, or the radius of a circular contact area, and k_c and k_ϕ denote cohesive and frictional pressure-sinkage parameters, respectively.

The soil classification defined by United States Department of Agriculture (USDA) textural triangle is used to obtain typical values for the characteristic parameters used in the pressure-sinkage relation. The USDA soil textural triangle is shown in Figure 2. At Sandia National Laboratories-Albuquerque NM, a device was developed to obtain the typical values for the characteristic parameters used in the pressure-sinkage relation as well as the shear stress-shear deformation relation that will be discussed shortly. The relations of a few homogenous and

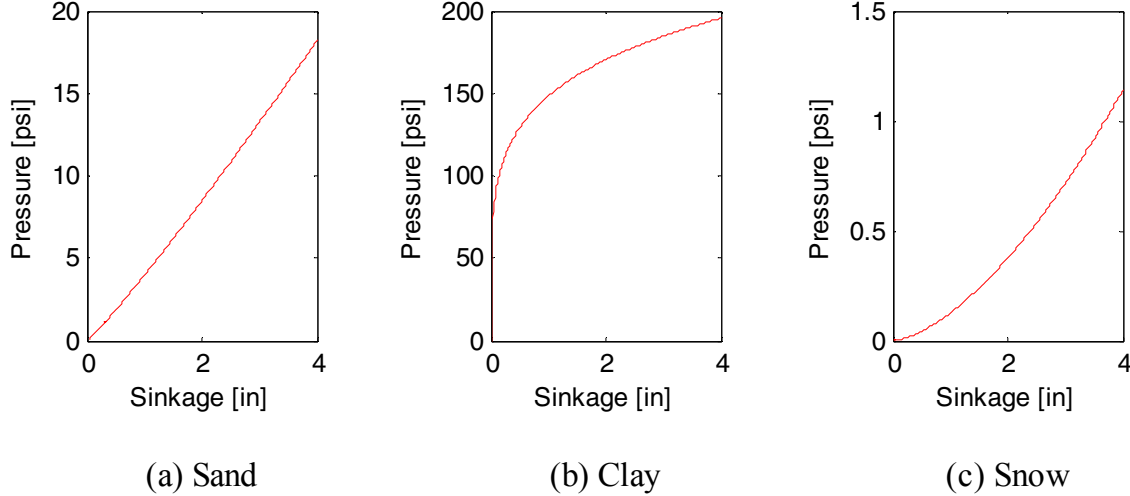


Figure 3: Pressure-Sinkage Relation of Various Homogeneous and Deformable Soils with 1.6 inch Penetration Plates

deformable soils are shown in Figure 3. For a relatively small sinkage, clay requires the largest pressure and snow requires the least pressure. However, pressure change in clay becomes smaller and smaller as sinkage increases, and the opposite is observed for snow.

3.4 Dissipation Energy Due to Deformation of Terrain

By borrowing the strain energy concept from mechanics in materials, the work done by a plate to create an indentation in a terrain can be estimated based on the pressure-sinkage relation. The work is given by:

$$Work = A_{plate} \int_0^{z_0} p_h(z) dz \quad (9)$$

where A_{plate} denotes the area of the plate, and z_0 denotes the depth of the indentation. By extending the idea, the dissipation energy for creating the track marks is given by:

$$E_{d,terrain} = bl \int_0^{z_0} p_h(z) dz \quad (10)$$

where b denotes width of the track mark which is same as the width of the tires; l denotes the length of the track mark which is same as the length of the path the vehicle travels; and z_0 denotes the depth of the track mark. In order to estimate the dissipation energy given in equation (10), the depth of the track mark must be known. When a track mark is created from the interaction between a wheel and a terrain, the depth of the track mark depends not only on the pressure-sinkage relation of the terrain, but also on the horizontal strength of the terrain because the wheel applies a radial stress as well as a shear stress on the contact surface of the terrain. There are several different ways to estimate the depth of the track mark. One is a direct measurement at the track mark. Another is an estimation of the track mark from sensor information. The other is an estimation of the track mark from the vertical force balance at the contact area between the tires and terrain. One can use any estimation method; however, the mobility algorithms use the vertical force balance approach to estimate the depth of the track

mark. Another relation, shear stress-shear deformation relation of terrain developed by Bekker is adopted for the force balance.

3.5 Shear Stress-Shear Deformation Relation of Homogenous and Deformable Terrain

Bekker [1] developed a shear stress-shear deformation relation of homogenous terrain. The relation describes the horizontal shear strength of the terrain for a given set of vertical stresses and shear stresses on the contact surface. The relation was developed by extending the Mohr-Coulomb criterion that is used to detect failure of a terrain when stresses are applied to the terrain. The criterion is widely accepted by the civil engineering community, and the criterion is given by:

$$\tau_{\max} = C + \sigma \tan(\phi) \quad (11)$$

where τ_{\max} denotes the maximum shear strength of the terrain for a given normal stress (σ) on the sheared surface, and C and ϕ denote the cohesion and the angle of internal shearing resistance of the terrain, respectively. The shear strength parameters, C and ϕ are measured from Mohr circles. When a terrain is subjected to different states of stress, a Mohr circle can be constructed for each mode of failure. Then, a straight line connecting the top of the Mohr circles is drawn. The shear strength parameters are calculated from the straight line. This is illustrated in Figure 4. The criterion is used to detect failure of a terrain if the shear stress is greater than the maximum shear stress computed from the criterion.

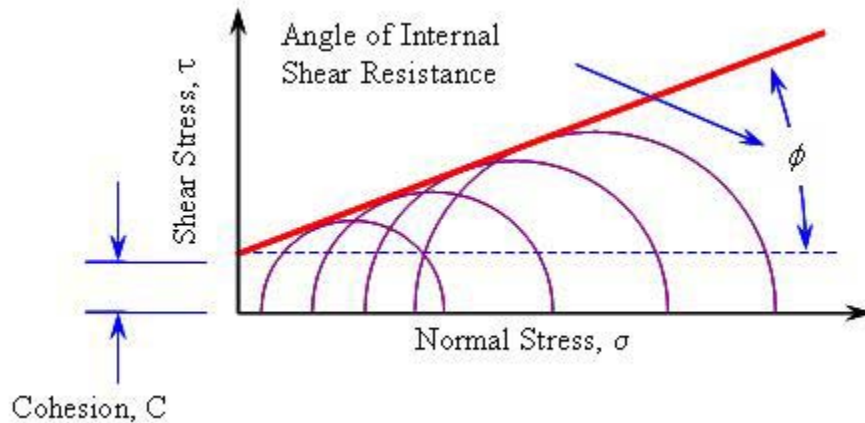


Figure 4: Mohr-Coulomb Soil Failure Criterion

A generally accepted approximation is found by Janosi and Hanamoto [3] who simplified the relation given by Bekker. Their approximation works well on most sands, saturated clay and fresh snow. The approximation is given by:

$$\tau = \tau_{\max} \left(1 - \exp\left(-\frac{J_{sd}}{K}\right) \right) \quad (12)$$

where τ denotes the shear stress function of the shear deformation (j_{sd}), and K denotes the shear deformation parameter. The value of K varies from 0.4 inch for a firm sandy terrain to 1.5 inches for loose sand, and the value is approximately 0.25 inch for clay at the maximum compaction. For undisturbed fresh snow, the value varies from 1 to 2 inches.

3.6 Distribution of Stresses at the Contact Area

There is no one description of the stresses at the contact area that satisfies everyone since the first description of the stresses published by Bekker [1] in 1956. Bekker developed analytic expressions for the distribution of tangential and radial stresses at the contact area using his pressure-sinkage and shear stress-shear deformation relations. Since then, many researchers modified Bekker's description.

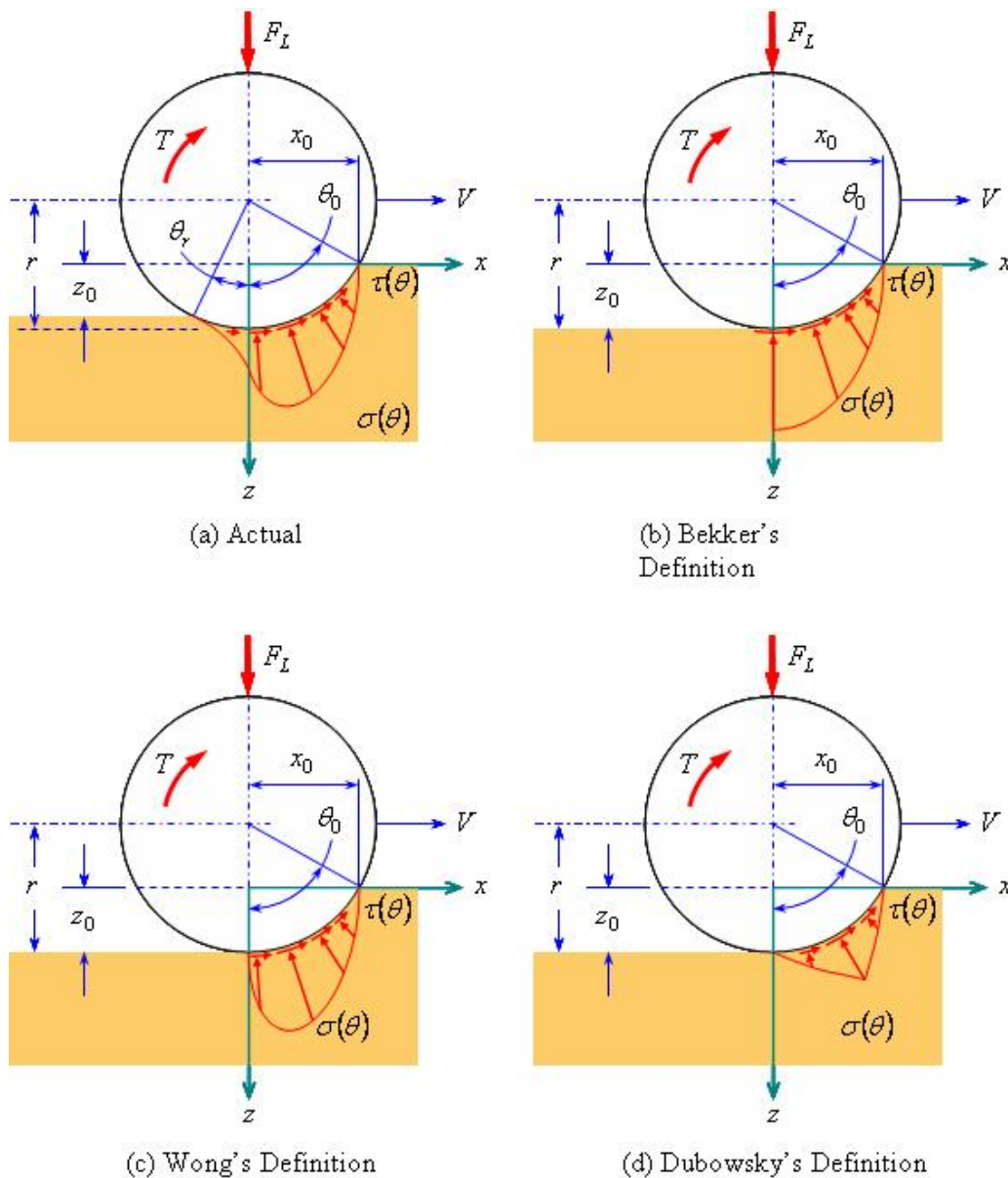


Figure 5: Description of Stresses Acting on Wheels

Wong and Reece [4 and 5] modified Bekker's expressions such that the maximum radial and tangential stresses are located at a point in the contact area. The location is given by a function of the slip of the tire. In a more recent year, Iagnemma and Dubowsky [6] simplified the Wong and Reece's expressions to make them computable for real-time estimation of the characteristic parameters used in the pressure-sinkage and shear stress-shear deformation relations. Figure 5 shows distribution of the stresses presented by them.

Like Wong and Dubowsky, we have developed a set of expressions for the distribution of the stresses, which was modified from Bekker's expressions for the mobility algorithms. The following description intends to give a basic demonstration of the analytical expressions used in the mobility algorithms. The distribution of the radial stress is defined as:

$$\sigma(\theta) = \begin{cases} k_s r^n [\cos(\theta) - \cos(\theta_0)]^n & , \theta_m \leq \theta \leq \theta_0 \\ k_s r^n \left[\cos\left(\theta_0 - \frac{\theta - \theta_r}{\theta_m - \theta_r} (\theta_0 - \theta_m)\right) - \cos(\theta_0) \right]^n & , \theta_r \leq \theta \leq \theta_m \end{cases} \quad (13)$$

Where s denotes the radial stress defined by a function of a contact angle (θ), r denotes radius of the wheel, and θ_0 , θ_r , and θ_m denote the angles from the vertical at which the tire makes contact with the terrain, breaks contact with the terrain, and creates the maximum radial stress, respectively. The radial stress gradually increases from the leading edge of the contact area to a certain point in the contact area, and then it gradually decreases to the trailing edge.

The location of the maximum radial stress is defined as:

$$\theta_m(i_s) = \begin{cases} (0.2 + 0.3i_s)\theta_0 & , i_s \geq 0 \\ \cos^{-1} \left[\frac{p_2 + p_1 \sqrt{p_1^2 + 1 - p_2^2}}{1 + p_1^2} \right] & , i_s < 0 \end{cases} \quad (14)$$

$$p_1 = \tan\left(\frac{\pi}{4} - \frac{\phi}{2}\right) \quad (15)$$

$$p_2 = \frac{1}{1 - i_s}$$

$$i_s = \frac{r\omega - V}{r\omega} \quad (16)$$

where i_s denotes the slip of the tire and it is defined in equation (16). The location depends on the slip. A positive slip means a driven wheel and a negative slip means a braked wheel. When a wheel is driven over a terrain, it is likely that some of the terrain deformation will recover as the wheel breaks off the contact with the terrain. This also depends on the amount of the wheel slip. The recovery angle of terrain is defined as:

$$\theta_r(i_s) = \begin{cases} 0.2i_s\theta_0 & , i_s \geq 0 \\ 0 & , i_s < 0 \end{cases} \quad (17)$$

The distribution of the tangential stress is defined as:

$$\tau(\theta) = \begin{cases} (C + \sigma(\theta)\tan(\phi))\left(1 - \exp\left(-\frac{J_{sd}}{K}\right)\right) & , i_s \geq 0 \\ -(C + \sigma(\theta)\tan(\phi))\left(1 - \exp\left(\frac{J_{sd}}{K}\right)\right) & , i_s < 0 \end{cases} \quad (18)$$

$$j_{sd}(i_s) = \begin{cases} r[(\theta_0 - \theta_m) - (1 - i_s)(\sin(\theta_0) - \sin(\theta))] & , i_s \geq 0 \\ r[(\theta_0 - \theta_m) - (1 - i_s)(\sin(\theta_0) - \sin(\theta)) + K_v(1 - i_s)(\theta_0 - \theta)] & , i_s < 0 \end{cases} \quad (19)$$

$$K_v(i_s) = \frac{(1 - i_s)(\sin(\theta_0) - \sin(\theta_m)) - (\theta_0 - \theta_m)}{(\theta_0 - \theta_m)(1 - i_s)} \quad (20)$$

The tangential stress depends on the radial stress and the shear deformation. The bulldozer effect on the terrain is added when the brake is applied.

3.7 Distribution of the Stresses Under Wheels in the Tandem Configuration

The multi-pass effect is one of the most important effects on the mobility analysis. It occurs when wheels in a tandem configuration travel a straight line path such that two or more wheels are traveling through the same rut. The stresses under wheels in the tandem configuration are shown in Figure 6. The radial reaction stress at the second wheel is larger than the one at the leading wheel due to the compaction of the terrain from the leading wheel. Because of this, the sinkage angle of the second wheel ($\theta_{0,2}$) is smaller than the sinkage angle of the leading wheel ($\theta_{0,1}$). The distribution of the radial stress at the i^{th} wheel is given by:

$$\sigma_i(\theta) = \begin{cases} k_s [r_i (\cos(\theta) - \cos(\theta_{0,i})) + z_p]^n & , \theta_m \leq \theta \leq \theta_0 \\ k_s \left\langle r_i \left[\cos\left(\theta_{0,i} - \frac{\theta - \theta_{r,i}}{\theta_{m,i} - \theta_{r,i}} (\theta_{0,i} - \theta_{m,i})\right) - \cos(\theta_{0,i}) \right] + z_p \right\rangle^n & , \theta_r \leq \theta \leq \theta_m \end{cases} \quad (21)$$

$$z_p = \sum_{j=1}^{i-1} r_j [\cos(\theta_{r,j}) - \cos(\theta_{0,j})] \quad (22)$$

where z_p denotes the compounded sinkage depth of the terrain that is created by the wheels in the tandem configuration up to the $(i-1)^{th}$ wheel. With minimum changes to equation (14) through equation (20), those relations are used for the i^{th} wheel.

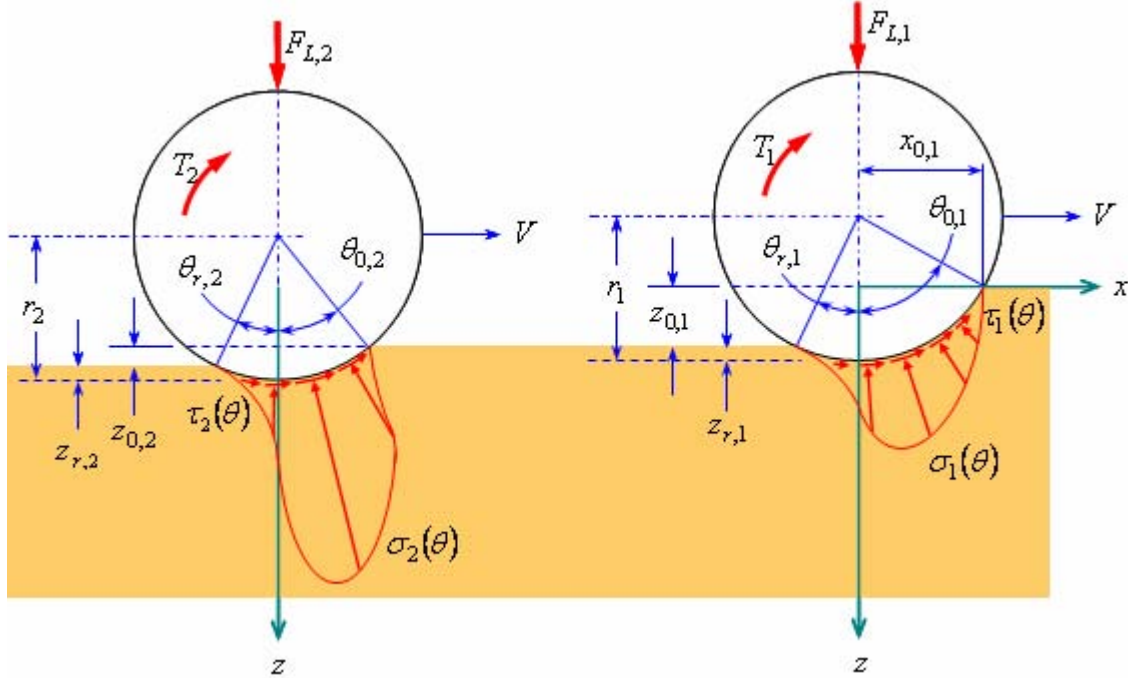


Figure 6: Stresses Acting on the Wheels in a Tandem Configuration

3.8 Depth of the Track Mark

With the distribution of the stresses defined the previous sections, the vertical force balance on the contact area at the i^{th} wheel is given by:

$$F_{L,i} = r_i b \int_{\theta_{r,i}}^{\theta_{0,i}} [\sigma_i(\theta, \theta_0) \cos(\theta) + \tau_i(\theta, \theta_0) \sin(\theta)] d\theta \quad (23)$$

Then, the depth of the track mark is given by:

$$z_0 = \sum_i z_{0,i} \quad (24)$$

$$z_{0,i} = r_i [\cos(\theta_{r,i}) - \cos(\theta_{0,i})]$$

where the index i , starts from 1 to the number of axles in the vehicle. The sinkage angle of each wheel $\theta_{0,i}$ must satisfy the vertical force balance relation given in equation (23).

3.9 Traction Energy Capability from Terrain

When a driving torque is applied to drive wheels of the traction system in a vehicle, a shearing stress is developed at the contact area of the tires/tracks and terrain. The traction energy

capability of the vehicle depends on the shear stress. Using the shear stress defined in equation (18), the traction energy capability of the vehicle is given by:

$$E_{tc,terrain} = \sum_i E_{tc,terrain,i} \quad (25)$$

$$E_{tc,terrain,i} = r_i b l \int_{\theta_{r,i}}^{\theta_{0,i}} \tau_i(\theta) d\theta$$

where j starts from 1 to the number of wheels in the vehicle.

3.10 Mobility Analysis Algorithms

In the previous sections, the energies involved in the operation of the vehicle over the soft and deformable terrain are identified, and analytical expressions are developed for the energies. Thus, the energy relation given in equation (6) can be rearranged to predict mobility of the vehicle over the terrain. In order to predict the maximum slope the vehicle can travel, equation (6) is rearranged as:

$$\theta = \sin^{-1} \left(\frac{E_{tc,terrain} - E_{d,terrain} - \frac{F_L}{2g} (v_f^2 - v_i^2)}{F_L l} \right) \quad (26)$$

where the dissipation energy is defined by equation (10) and the traction energy capability is defined by equation (25). In order to predict whether the vehicle can travel over the terrain or not, the equation (6) is rearranged as:

$$v_f^2 = v_i^2 + \frac{2g}{F_L} [E_{tc,terrain} - E_{d,terrain} - F_L l \sin(\theta)] \quad (27)$$

If the right hand side of equation (27) is positive, then the vehicle can travel over the terrain. Otherwise, it cannot travel over the terrain.

4 Mobility Analysis Tool

The mobility analysis tool is a graphical user interface (GUI) application that is user-friendly, computationally efficient and laptop portable. A user can interact with the GUI to pass necessary information to the mobility analysis algorithms module, and to see results of the analysis on the GUI display panel. In this section, the functions included in the tool are described.

4.1 Overall Picture

When the mobility analysis tool is started, the tool will be displayed on the desktop window. The tool will be loaded with default information about the vehicle and terrain such that a user can start to analyze mobility of a vehicle without entering any information. A snapshot of the mobility analysis tool is shown in Figure 7. The tool contains menus on the top of the application window and two main panels (input on the left side and display on the right). The

input panel has 2 sub-panels; information on the top and command on the bottom. The information panel is used to select/enter/modify characteristic information of the terrain, obstacle, and vehicle. The command panel contains two buttons at the bottom that perform given actions when they are pushed.

The display panel also has 2 sub-panels; graphics on the top and status on the bottom. The graphics panel has multiple functions. It can be used to display a mobility analysis result, useful descriptions about the characteristic information of vehicles, terrain and obstacles, and general information about the tool. Figure 8 shows typical mobility prediction results. The status panel is used to display information about the current status of the tool. It is also used to display helpful hints about certain operations of the tool.

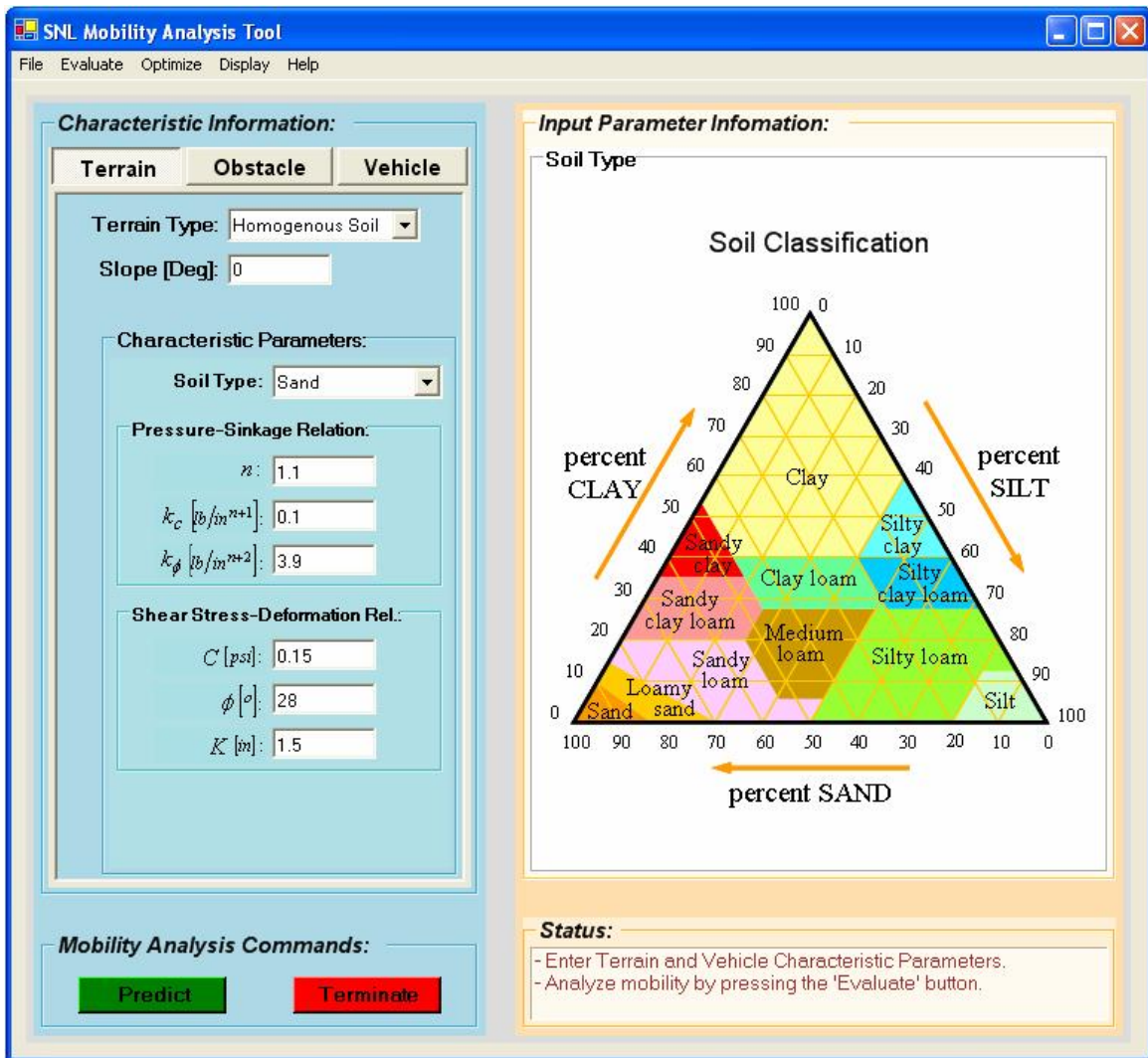
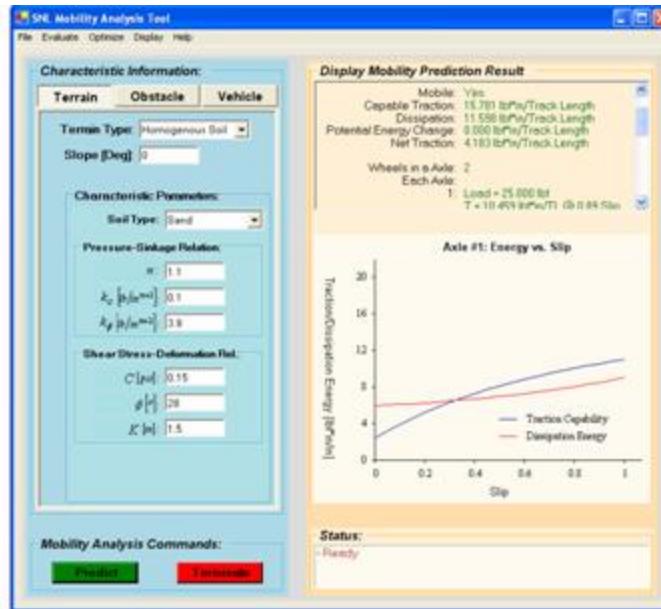
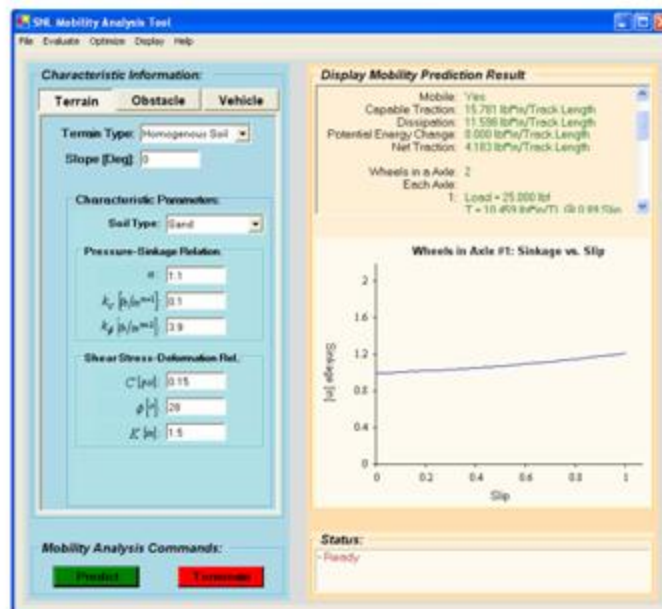


Figure 7: Mobility Analysis Tool at Startup



(a) Traction energy capability and dissipation energy display



(b) Sinkage display

Figure 8: Mobility Analysis Tool Showing Mobility Prediction Display

(a) Terrain Tab

(b) Vehicle Tab

Figure 9: Tabs in the Input Panel (Obstacle Tab Not Enabled)

4.2 The Input Panel

The input panel contains three tabs: the terrain tab, obstacle tab and vehicle tab. Each tab allows a user to define characteristic information of terrain, vehicle and obstacles for the mobility analysis. The contents of terrain and vehicle tabs are shown in Figure 9.

4.2.1 Defining Terrain Characteristic Parameters

A user can select a type of terrain from the drop-down box. When a terrain is chosen, a set of appropriate characteristic parameters will be shown in the panel. In the current version of the mobility tool, only homogenous soil is enabled for the terrain type. The information of the characteristic parameters is available from the 'Help' menu. The user can display the information on the display panel by selecting a menu item from the 'Help/Input Information' menu. For homogeneous soils, the user can select a type of soil classified by the United States Department of Agriculture (USDA) from the drop-down box. When a soil is chosen, a typical value of the characteristic parameters will be displayed in the text box next to the text label of a parameter. At this point, a user can accept these values or modify them in the text box.

4.2.2 *Defining Obstacle Characteristic Parameters*

A user can select a type of obstacle from the drop-down box. When an obstacle is chosen, a set of appropriate characteristic parameters will be shown in the panel. In the current version of the mobility tool, none of the obstacles are enabled.

4.2.3 *Defining Vehicle Characteristic Parameters*

A user can select a type of vehicle from the drop-down box. When a vehicle is chosen, a set of appropriate characteristic parameters will be shown in the panel. In the current version of the mobility tool, only a rigid wheel is enabled for the vehicle type. The information of the characteristic parameters is available from the 'Help' menu. The user can display the information on the display panel by selecting a 'Vehicle Characteristic Parameter' menu item from the 'Help/Input Information' menu. The user can select a number of axles from the drop-down box. Then, the user must select an axle identification (ID) number from the drop-down box in order to see the values for the characteristic parameters as well as to modify them. The axle ID number 1 corresponds to the leading wheel. When an axle ID is chosen, a default value of the characteristic parameters will be displayed in the text box next to the text label of a parameter. At this point, a user can accept these values or modify them in the text box. If the check-mark box next to the text box is checked, then the value in the text box will be applied to all axles.

4.3 *Menu items*

There are five main menus in the mobility analysis tool. They are 'File' menu, 'Evaluate' menu, 'Optimize' menu, 'Display' menu and 'Help' menu. The main menus can be seen from Figure 7. The structure of the menus and the function of each item are shown below:

- 'File' menu
 - 'Load Characteristic Information': The menu is used to load characteristic information of terrain, obstacle and vehicle from files, i.e. drawing files from SolidWorks, image files from satellite pictures, etc. This function is not available yet.
 - 'Load data from file' and 'Save data to file': The items are used to load and save data from mobility analysis result into a data file.
 - 'Terminate': The item is used to terminate the application. The same action can be achieved by pushing the 'Terminate' button in the command panel.
- 'Evaluate' menu
 - 'Predict Mobility': The item is used to estimate the mobility capabilities of the vehicle over the terrain that is defined in the input panel. The same action can be achieved by pushing the 'Predict' button in the command panel.
 - 'Maximum Negotiable Terrain Slopes vs. Vehicle Loads': The item is used to estimate the maximum slope of terrain the vehicle can travel as a function of the vehicle load.
- 'Optimize' menu: Optimize characteristic parameters of the vehicle in order to achieve the maximum mobility performance (net traction energy).
 - 'One Parameter': Optimize one characteristic parameter of the vehicle in order to achieve the maximum mobility performance (net traction energy).
 - 'Center of Gravity':
 - 'x': Optimize the center of gravity in the longitudinal direction.

- 'y': Optimize the center of gravity in the vertical direction.
 - 'Vehicle Load': Optimize the vehicle load.
 - 'Wheel Radius': Optimize the radius of the wheels.
 - 'Wheel Width': Optimize the width of the wheels.
 - 'Multi Parameter': Optimize multiple characteristic parameters of the vehicle in order to achieve the maximum mobility performance (net traction energy). This function is not available yet.
- 'Display' menu
 - 'Mobility Result':
 - 'Summary': The item is used to display the summary of the mobility analysis result in a text form.
 - 'In Graphic': The items in this menu are used to display the dissipation energy and the traction energy capability of each axle in a graphic form.
 - 'Sinkage': The items in this menu are used to display the sinkage of each wheel in graphic form.
 - 'Radial and Tangential Stresses': The items in this menu are used to display the stress distribution at each wheel in a graphic form.
 - 'Optimization Result':
 - 'Summary': The item is used to display the summary of the optimization result in a text form.
 - 'In Graphic': The items in the menu are used to display the optimization result in a graphic form.
 - 'Terrain Characteristics': The items in the menu are used to display the pressure-sinkage and shear stress-shear deformation relations of the terrain given in the input panel.
 - 'Maximum Negotiable Terrain Slopes vs. Vehicle Load': The item is used to display the result of the 'Maximum Negotiable Terrain Slopes vs. Vehicle Load' from the 'Evaluate' main menu.
- 'Help' menu
 - 'About the Tool': The item is used to display brief information about the tool.
 - 'Input Information':
 - 'Soil Type': The item is used to display the soil textual triangle defined by United States Department of Agriculture (USDA).
 - 'Terrain Characteristic Parameters': The item is used to display a brief description about the terrain characteristic parameters used in the input panel.
 - 'Vehicle Characteristic Parameters': The item is used to display a brief description about the vehicle characteristic parameters used in the input panel.

5 Conclusion

Predicting the mobility capability of ground robotic vehicles over general terrain is a largely unsolved problem. A better, more robust solution to this problem is important for the proper selection of vehicle configuration and design parameters to meet specific operational requirements. This also correlates directly with optimizing vehicle operations relating to the probability of mission success, power dissipation, time to accomplish missions, and the selection

of vehicles themselves. This paper describes an ongoing effort to develop a tool to analyze the mobility of robotic ground vehicles (large and small scale) over general terrain based on the principle of conservation of energy. The framework of the tool and the analysis behind it were shown and a few sample results discussed. These results were consistent with the intuitive understanding of ground vehicle mobility over a given terrain. However, the results were not validated through hardware demonstrations. Future work will include a demonstration of the accuracy of the mobility analysis through experimentation. Furthermore, analytic expressions will be developed for more heterogeneous terrains with mixed soils, solids such as rocks, urban environment debris, and vegetation, and for tracked or legged robotic ground vehicles.

6 References

- [1] Bekker, M.G., *Theory of Land Locomotion*, University of Michigan Press, Ann Arbor, MI, 1956.
- [2] Bekker, M.G., *Introduction to Terrain-Vehicle Systems*, University of Michigan Press, Ann Arbor, MI, 1969.
- [3] Janosi, Z., and Hanamoto, "Analytical determination of drawbar pull as a function of slip for tracked vehicles in deformable soils," *Proceedings of the First International Conference on Terrain-Vehicle Systems*, Edizioni Minerva Tecnica, Torino, 1961.
- [4] Wong, J.Y., and Reece, A.R., "Prediction of rigid wheel performance based on the analysis of soil-wheel stresses - Part I. Performance of driven rigid wheel," *Journal of Terramechanics*, vol. 4, no. 1, pp. 81-98, 1967.
- [5] Wong, J.Y., and Reece, A.R., "Prediction of rigid wheel performance based on the analysis of soil-wheel stresses - Part II. Performance of towed rigid wheels," *Journal of Terramechanics*, vol. 4, no. 2, pp. 7-25, 1967.
- [6] Iagnemma, K., and Dubowsky, S., "Terrain estimation for high-speed rough-terrain autonomous vehicle navigation," *Proceedings of SPIE Conference on Unmanned Ground Vehicle Technology IV*, vol. 4715, pp. 256-266, 2002.
- [7] Haueisen, Brooke, "Mobility Analysis of Small, Lightweight Robotic Vehicles," Project Report # 6807 9990, April 25, 2003.

7 **Distribution**

1	MS 1003	John Feddema, 6473
1	MS 1125	Scott Gladwell, 6472
1	MS 1003	Scott Horschel, 6473
1	MS 1009	David Novick, 6474
1	MS 1003	Jon R. Salton, 6473
1	MS 1003	Barry Spletzer, 6470
2	MS 9018	Central Technical Files, 8944
2	MS 0899	Technical Library, 9536